Supplementary Information

Using DILIsym to investigate observed species differences in CKA-mediated hepatotoxicity

Christina Battista, Kyunghee Yang, Simone H. Stahl, Jerome T. Mettetal, Paul B Watkins, Scott Q Siler, Brett A Howell

Corresponding author: Brett A. Howell

Current address: Six Davis Drive, Research Triangle Park, NC 27709

E-mail address: bhowell@dilisym.com

Telephone: 919-558-1323, Fax: N/A

METHODS

Physiologically-based pharmacokinetic (PBPK) model development

CKA was represented in the PBPK submodel which consists of a central blood compartment, as well as hepatic, muscle, gut, and other tissues linked to the central compartment via blood flow. The liver, consisting of three zones, is represented with the same density of hepatocytes in each zone, and each zone (the centrilobular, midlobular, and periportal) accounts for 1/9, 3/9, and 5/9 of the total liver volume, respectively. Following the direction of blood flow, compounds move from the periportal zone to the midlobular zone to the centrilobular zone and ultimately end up in the blood compartment. Glucuronidation of CKA was represented using saturable Michaelis-Menten kinetics, while hepatic uptake and biliary clearance were linear functions. There were no data to support active uptake of CKA into hepatocytes. As such, CKA disposition was mediated by passive diffusion, and because plasma concentration is closely tied to compound clearance, liver concentration predictions were assumed reasonable due to the liver's function as a major clearance organ. Additional details on the PBPK submodel in DILIsym are given in the supplementary material in Woodhead *et al.*[1] and Howell *et al.*[2] Physiological parameters for tissue volumes and blood flows in the PBPK submodel of DILIsym are found in the supplementary material in Howell *et al.*[2] Upon retrospective analysis performed after optimization of the PBPK model, partition coefficients defining tissue distribution were compared to *in silico* predictions from GastroPlus and Rodgers and Rowland[3] and found to be reasonable. Because CKA is highly bound to plasma proteins and measurement errors were assumed, the fraction unbound had to be included in the optimization scheme and therefore *in silico* predictions of these partition coefficients could not be utilized in the construction of the PBPK model but were rather used as comparison after fraction unbound values were predicted.

Determination of ETC (electron transport chain) inhibition parameter values for CKA

HepG2 cells were incubated with 0–750 µM (6 concentrations) CKA for 6 hours. Oxygen consumption rate (OCR) was measured using a Seahorse XFe24 Analyzer (Agilent Technologies, Santa Clara, CA).[4] Protein content was measured using the Pierce BCA protein assay (ThermoFisher Scientific, Waltham, MA) to estimate cell count, and measured OCR

values were adjusted to account for cell viability. Parameter values for CKA-mediated ETC inhibition (ETCi) were determined in MITOsym®, a mitochondrial modeling platform used to reproduce *in vitro* experimental results,[5] by fitting simulated results to changes in OCR data subsequent to CKA administration. The same mechanistic descriptions of mitochondrial pathways are included in MITOsym and DILIsym, with DILIsym incorporating additional descriptions to account for *in vivo*-only representations. Conversion factors were used to translate predicted results from HepG2 cells to human and rat hepatocytes based on existing literature, and the resulting MITOsym ETCi parameters were then converted to DILIsym parameters.[6]

Determination of reactive oxygen species (ROS) production parameter values for CKA

Formation of ROS was assessed by high content screening using the fluorescent probe dihydroethidium (DHE) as a measure of oxidative stress.[7] Briefly, HepG2 cells were plated onto black, clear-bottom 96-well plates. After incubation with 0–750 µM (8 concentrations) CKA for 6 or 24 hours, DHE was added and the plate was scanned using an ArrayScan™ (ThermoFisher Scientific, Waltham, MA). The cellular ATP content was measured using CellTiter-Glo® (Promega, Madison, WI). Oxidative stress assays were performed by Cyprotex Discovery Limited (Macclesfield, UK). DILIsym was used to determine the rate at which CKA mediates oxidative stress (or ROS production) by creating an *in vitro*-like scenario, accomplished using IV infusion dosing to create a constant liver concentration which mimics that of the *in vitro* environment. The ROS production constant parameter was found by sweeping through potential values until the simulation yielded ROS effects in line with the measured data.

Determination of bile acid (BA) transporter inhibition parameter values for CKA

The published half-maximal inhibitory concentration (IC_{50}) value of CKA for rat BSEP was used to represent the inhibition constant (K_i) in DILIsym.[8] IC_{50} values for human MRP3, MRP4 were determined in transporter-overexpressing vesicles and for NTCP in transfected cell lines which were then used to represent inhibition constants in DILIsym (shown in **Table 1**). CKA caused concentration-dependent inhibition of [3H]taurocholate uptake by membrane vesicles that expressed human BSEP.[8] CKA also concentration-dependently inhibited the MRP3-mediated transport of β-estradiol-17-β-D-glucuronide ($E_2$17βG), the MRP4-mediated transport of dehydroepiandrosterone sulphate (DHEAS), and NTCP-mediated uptake of taurocholate into the vesicles. MRP3, MRP4, and NTCP transporter inhibition assays were performed by Solvo® Biotechnology (Budaörs, Hungary). DILIsym currently uses a single K_i for basolateral efflux transport, and thus the more potent basolateral inhibition value was used to model CKA, i.e. the IC_{50} for MRP3 instead of MRP4. For transporters where data were lacking, the same IC_{50} value was assumed across species because human and rat BSEP transporter IC_{50} values were similar.[9] Details on the BA submodel in DILIsym can be found in the supplementary material in Woodhead *et al.*[10] Because the modes of inhibition were not determined, the most potentially toxic scenario was simulated (competitive inhibition for NTCP and non-competitive inhibition for BSEP and MRP3).[11,12]

Determining intracellular concentration in *in vitro* assays

Although *in vitro* assay data can provide straightforward, valuable insight into possible toxicity mechanisms, toxicity is ultimately dependent upon the exposure determined by the intracellular concentration of a compound, and therefore intracellular concentration must be considered when accurately predicting toxicity outcomes.[13] When intracellular concentration is not measured, the simplest, but most errant, estimation method, termed the *nominal assumption*, is to assume that total and free extracellular concentrations are the same as total and free intracellular concentrations. However, this is rarely a true representation of reality. Instead, intracellular concentration can be estimated by accumulation (or scaling) factors, dependent upon the experimental protocol and determined by partition coefficients.[14] For protein-free media assays, the accumulation factor $K_{p,u}$, the tissue-to-plasma partition coefficient based on the unbound concentration, should be used because there is less protein to which the compound can bind, and it is assumed that the total extracellular concentration represents the unbound intracellular concentration. Conversely, for assays performed in media with protein, the scaling factor used is K_p, the tissue-to-plasma partition coefficient based on total concentration, since there are more proteins to which the compound can bind so both unbound and bound concentrations in the media are accounted for in this factor. In both scenarios, the intracellular concentration is estimated as the product of the accumulation factor and the extracellular (or media) concentration.

Rodgers and Rowland[3,15] calculate K_p and $K_{p,u}$ based on properties of the compound, i.e. fraction unbound in plasma, pH, pK_a, and blood-to-plasma ratio. Alternatively, K_p and $K_{p,u}$ can be estimated from PBPK model simulations as the ratio of liver C_{max} to plasma C_{max}, noting that the correct (total or unbound) plasma concentration is used. However, to accurately mimic an *in vitro* environment, this ratio should be calculated at steady state. For this study, the physiologically-based pharmacokinetic (PBPK) model of CKA was used with two dosing schemes to estimate the accumulation factors; oral dosing and IV infusion dosing were implemented. The IV infusion dosing scheme was tuned such that the same peak plasma exposure levels as those in the preclinical and clinical trials were simulated by the PBPK model. This work assumes that the latter (IV infusion dosing) more closely imitates an *in vitro*-like environment at steady state, and thus the accumulation factors resulting from this model are used throughout this study.

RESULTS

Investigating CKA toxicity mechanism sensitivity

As outlined in the main text, *in vitro* data indicate that CKA increases reactive oxygen species (ROS) production, inhibits electron transport chain (ETC) activity, and inhibits bile acid (BA) transport. Qualitative and quantitative approaches were taken to determine which toxicity mechanism CKA is most sensitive to.

Under the qualitative approach, all possible permutations of the active toxicity mechanisms (ROS production, mitochondrial toxicity, and BA transporter inhibition) were simulated in the human and rat SimPops with 900 mg and 500 mg/kg doses, respectively. Each mechanism was studied individually, noting that mitochondrial toxicity via ETC inhibition appeared to be the only mechanism causing an increase in serum ALT by itself in the rat population. ETC inhibition leads to a disruption in the proton gradient, ultimately reducing adenosine triphosphate (ATP) synthesis and increasing heat production. Different combinations of two mechanisms

were then activated in the model, and the simulation results were qualitatively analyzed (**Figure 4**). Through this analysis, the primary contributor to CKA rat hepatotoxicity was ETC inhibition with BA transporter inhibition also contributing to a lesser extent as the secondary mechanism. ROS production appeared to contribute minimally to elevations in serum ALT in the rat population. Serum ALT levels did not significantly increase in the human simulated population for any combination of toxicity mechanisms.

A more quantitative approach, a multiple linear regression analysis, was performed using the rat SimPops results to statistically ensure that mitochondrial toxicity was, in fact, the main contributing mechanism to CKA hepatotoxicity. In the analysis, maximum serum ALT level was deemed the dependent variable, while the parameters that varied in the rat SimPops were assigned as the independent variables. The statistical significance of each rat SimPops parameter on ALT elevation is shown in **Supplementary Table S2**. Only one parameter was a statistically significant predictor of serum ALT levels, the basal value of the standardized ETC flux (**Supplementary Figure S1**). Notably, the basal value of the standardized ETC flux parameter is within the mitochondrial toxicity submodel,[6,16] thus supporting ETC inhibition as the main contributor to CKA-mediated rat hepatotoxicity. Three additional parameters had small P-values, although they did not meet the statistical significance threshold at $P < 0.001$. Two of these parameters, the scaling coefficient for representing the amount of reserve mitochondrial ETC function and the maximum rate of bulk bile acid canalicular transport, are found within the mitochondrial toxicity and BA homeostasis submodels, respectively. This suggests that while ETC inhibition is the main contributor to CKA toxicity, BA accumulation is likely the secondary contributor at supratherapeutic doses. The third parameter with a small p-value was the maximum reaction rate between ATP decrement and necrosis, which is included to mimic variation found throughout a species population. It is interesting that this parameter has a small p-value since it is not associated with any of the toxicity mechanisms, but rather provides variation in the population itself, suggesting that certain simulated rats are more naturally prone to CKA-mediated hepatotoxicity.

CKA intracellular adjustment for *in vitro* assays

Intracellular concentration of CKA was not measured in either of the assays used to determine hepatotoxicity due to reactive oxygen species (ROS) generation or mitochondrial toxicity. The approach taken herein based the estimated intracellular concentration on the experimental protocol used, i.e. estimates were dependent upon whether the assay was performed in media with or without protein. In this study, K_p and $K_{p,u}$ values were determined by three methods: the method suggested by Rodgers and Rowland[3,15], PBPK simulations with oral dosing, and PBPK simulations with IV infusion dosing. Final results predicting hepatotoxicity used the values calculated based on the scaling factor from the human PBPK model for CKA with IV infusion dosing. The human PBPK model was used rather than the rat PBPK model because the assays of interest (ROS and Seahorse XF) were performed in HepG2 cells which more closely resemble human hepatocytes than rat hepatocytes. Additionally, IV infusion dosing is more representative of the *in vitro* environment at steady state than the dynamical changes associated with oral dosing. Calculated values for K_p and $K_{p,u}$ from each method are shown in **Supplementary Table S3**. Regarding the estimations for human K_p and $K_{p,u}$, the PBPK IV infusion and Rodgers and Rowland methods are comparable.

In investigating CKA-mediated toxicity, the Seahorse XF assay was performed in protein-free media. The ROS assay was performed in media with protein. Both datasets were adjusted from extracellular concentrations to their respective intracellular concentrations (via scaling factor $K_{p,u}$ for the Seahorse XF assay and K_p for the ROS assay) and the corresponding DILIsym® parameters were found. However, as previously discussed, mitochondrial toxicity was the primary mechanism driving CKA-mediated toxicity. The electron transport chain (ETC) inhibition parameter is dependent upon which intracellular concentration assumption is used, and sensitivities to this parameter are shown in **Supplementary Figure S2**. Notably, both the nominal and K_p-adjusted concentration assumptions overestimate alanine transaminase (ALT) increases while the $K_{p,u}$-adjusted concentration assumption (which was used in the final results) is more accurate in reproducing the preclinical observations. Furthermore, the K_p-adjusted and nominal concentrations also predicted 100% of the rat population with serum ALT >10x upper limit of normal. With the $K_{p,u}$-adjusted assumption, viable liver mass ranged from 47 – 100%, but the K_p-adjusted and nominal concentration assumptions predicted that the majority (100% and 91%, respectively) of rats had less than 15% viable liver mass, signaling death in the simulation (**Supplementary Figure S2**).

References

1. Woodhead JL, Howell BA, Yang Y, Harrill AH, Clewell HJ 3rd, Andersen ME, et al. An analysis of N-acetylcysteine treatment for acetaminophen overdose using a systems model of drug-induced liver injury. J Pharmacol Exp Ther. 2012 Aug;342(2):529–40.

2. Howell BA, Yang Y, Kumar R, Woodhead JL, Harrill AH, Clewell HJ 3rd, et al. In vitro to in vivo extrapolation and species response comparisons for drug-induced liver injury (DILI) using DILIsym™: a mechanistic, mathematical model of DILI. J Pharmacokinet Pharmacodyn. 2012 Oct;39(5):527–41.

3. Rodgers T, Rowland M. Physiologically based pharmacokinetic modelling 2: predicting the tissue distribution of acids, very weak bases, neutrals and zwitterions. J Pharm Sci. 2006;95(6):1238–57.

4. Eakins J, Bauch C, Woodhouse H, Park B, Bevan S, Dilworth C, et al. A combined in vitro approach to improve the prediction of mitochondrial toxicants. Toxicol In Vitro. 2016 Aug;34:161–70.

5. Yang Y, Nadanaciva S, Will Y, Woodhead JL, Howell BA, Watkins PB, et al. MITOsym®: A Mechanistic, Mathematical Model of Hepatocellular Respiration and Bioenergetics. Pharm Res. 2015 Jun;32(6):1975–92.

6. Yang Y, Nadanaciva S, Will Y, Woodhead JL, Howell BA, Watkins PB, et al. MITOsym®: A Mechanistic, Mathematical Model of Hepatocellular Respiration and Bioenergetics. Pharm Res. 2014 Dec 12;

7. Woodhead JL, Brock WJ, Roth SE, Shoaf SE, Brouwer KLR, Church R, et al. Application of a Mechanistic Model to Evaluate Putative Mechanisms of Tolvaptan Drug-Induced Liver Injury and Identify Patient Susceptibility Factors. Toxicol Sci. 2017 Jan;155(1):61–74.

8. Ulloa JL, Stahl S, Yates J, Woodhouse N, Kenna JG, Jones HB, et al. Assessment of gadoxetate DCE-MRI as a biomarker of hepatobiliary transporter inhibition. NMR Biomed. 2013 Oct;26(10):1258–70.

9. Yang K, Woodhead JL, Watkins PB, Howell BA, Brouwer KL. Systems Pharmacology Modeling Predicts Delayed Presentation and Species Differences in Bile Acid-Mediated Troglitazone Hepatotoxicity. Clin Pharmacol Ther. 2014 Jul 28;589–98.

10. Woodhead JL, Brock WJ, Roth SE, Shoaf SE, Brouwer KLR, Church R, et al. Application of a Mechanistic Model to Evaluate Putative Mechanisms of Tolvaptan Drug-Induced Liver Injury and Identify Patient Susceptibility Factors. Toxicol Sci Off J Soc Toxicol. 2016 Sep 21;

11. Woodhead JL, Yang K, Siler SQ, Watkins PB, Brouwer KLR, Barton HA, et al. Exploring BSEP inhibition-mediated toxicity with a mechanistic model of drug-induced liver injury. Front Pharmacol. 2014;5:240.

12. Yang K, Pfeifer ND, Köck K, Brouwer KLR. Species differences in hepatobiliary disposition of taurocholic acid in human and rat sandwich-cultured hepatocytes: implications for drug-induced liver injury. J Pharmacol Exp Ther. 2015 May;353(2):415–23.

13. Groothuis FA, Heringa MB, Nicol B, Hermens JLM, Blaauboer BJ, Kramer NI. Dose metric considerations in in vitro assays to improve quantitative in vitro-in vivo dose extrapolations. Toxicology. 2015 Jun 5;332:30–40.

14. Chu X, Korzekwa K, Elsby R, Fenner K, Galetin a, Lai Y, et al. Intracellular drug concentrations and transporters: measurement, modeling, and implications for the liver. Clin Pharmacol Ther. 2013 Jul;94(1):126–41.

15. Rodgers T, Leahy D, Rowland M. Physiologically based pharmacokinetic modeling 1: predicting the tissue distribution of moderate-to-strong bases. J Pharm Sci. 2005 Jun;94(6):1259–76.

16. Woodhead J, Yang K, Yang Y, Howell B, Siler S. Understanding the Interaction between Hepatic Bile Acid Accumulation and Mitochondrial Toxicity Using Mechanistic Modeling. In: Abstracts Accepted for American Conference on Pharmacometrics 2014 (ACoP5). Las Vegas, NV: J Pharmacokinet Pharmacodyn; 2014. p. S30.

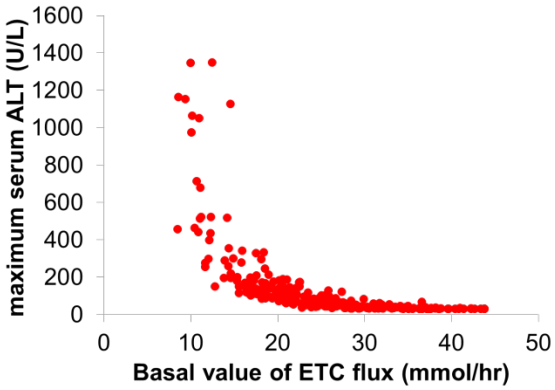

Supplement Figure S1. Correlation between maximum serum ALT and the basal value of ETC flux. The basal value of ETC flux, a parameter in the mitochondrial toxicity submodel, was significantly associated with CKA-mediated hepatotoxicity. This was the only SimPops parameter varied that reached statistical significance ($P < 0.001$) in a multiple regression analysis performed to identify the main contributor(s) in CKA toxicity (**Table S3**). A clear relation between lower values in the basal value of ETC flux and an increase in maximum serum ALT is observed.

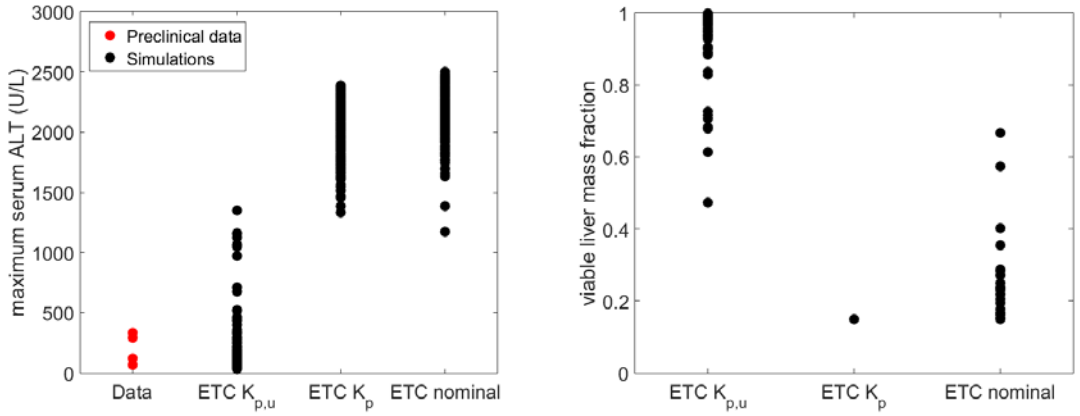

Supplement Figure S2. Sensitivity analysis to intracellular concentration assumption. Serum alanine transaminase (ALT) and viable liver mass fraction sensitivities to the electron transport chain (ETC) inhibition parameter based on the intracellular concentration assumption in rats. For this particular study, the Seahorse XF assay was performed in protein-free media, and thus $K_{p,u}$ is used as the accumulation factor to estimate intracellular concentration. When the K_p-adjusted or nominal concentration assumptions are used to estimate the intracellular concentration, the ETC inhibition parameter decreases, making CKA appear to be more potent. Serum ALT levels with the K_p-adjusted and nominal concentration assumptions are much higher than those observed in preclinical trials and result in a smaller fraction of viable liver.

Supplement Table S1. Drug-dependent PBPK input parameters for human and rat CKA simulations.

PBPK Input Parameters				
Parameter	Units	Human value	Rat value	Methods/References
Molecular weight	g/mol	369.72	369.72	AZ
Log P	n.d.	4.98	4.98	AZ
pKa	n.d.	3.7	3.7	AZ
Blood to plasma total concentration ratio	n.d.	1.2	1.2	assumed
Biliary clearance of CKA	mL/hr/kg^0.75	750	572.4551	Parameter estimation†
Gut to blood partition coefficient	n.d.	0.021848	2.403846	Parameter estimation†
Liver to blood partition coefficient	n.d.	0.184959	0.479294	Parameter estimation†
Muscle to blood partition coefficient	n.d.	0.076368	0.344923	Parameter estimation†
Other tissues to blood partition coefficient	n.d.	28.4137	1.29668	Parameter estimation†
Fraction of the CKA unbound in plasma	n.d.	0.0091 (0.0023)	0.0375	Parameter estimation† (AZ)
Renal clearance of CKA	mL/hr/kg^0.75	5.9151	268.7072	Parameter estimation†
Absorption from gut Vmax (maximum velocity of absorption from gut)	1/hr	123.8546	204.7940	Parameter estimation†
Absorption from gut Km (Michaelis-Menten constant of absorption from gut)	1/hr	19.9977	19.7398	Parameter estimation†
Km glucuronidation of CKA (Michaelis-Menten constant of CKA metabolism)	mol/mL	2.4521e-6	0.005	Parameter estimation†
Vmax glucuronidation of CKA (maximum velocity of CKA metabolism)	mol/hr/kg^0.75	8.1381e-5	8.1905e-4	Parameter estimation†
Fraction of CKA that is enterohepatically recirculated	n.d.	1	0.9664	Parameter estimation†
Rate of elimination of CKA in feces	1/hr	5.1545	0.7783	Parameter estimation†
Rate of CKA gastric emptying into the gut lumen	1/hr	12.1149	140.4617	Parameter estimation†
Rate of CKA absorption from the gut lumen to gut tissue	1/hr	2.3144	14.355	Parameter estimation†
Rate of absorption into the gut tissue for CKA glucuronide during enterohepatic recirculation	1/hr	10.8645	3.7806	Parameter estimation†
Fraction of CKA glucuronide that is enterohepatically recirculated	n.d.	0.2086	0.3391	Parameter estimation†
Rate of CKA dissolution	1/hr	12	726.2086	Parameter estimation†

Due to lack of data, most parameters were optimized to match simulated plasma concentrations to observed plasma concentrations. AZ indicates values provided by AstraZeneca.

†Optimized using CKA plasma concentration versus time data

n.d. non-dimensional

Supplement Table S2. Parameters varied in human and rat SimPops. Human and rat population samples incorporating variability in parameters governing bile acid (BA) homeostasis, reactive oxygen species (ROS) generation, and mitochondrial function have been previously constructed. Unless otherwise specified, the parameter appears in both human and rat SimPops. Results of multiple regression analysis signifying most important parameters contributing to hepatotoxicity in rat SimPops for 500mg/kg single dose.

DILIsym® Parameter	Parameter Description	Units	Significance
	Mitochondrial toxicity submodel		
Basal_Stdzd_MitoETC_Flux	Basal value of mito ETC flux	mmol/hr	P < 0.0001
Resp_Reserve_Scalar	Scaling coefficient for the amount of reserve mitochondria ETC function	n.d.	NS (P = 0.0222)
	Bile acid homeostasis submodel		
BA_baso_Vmax	Maximum rate of bulk bile acid basolateral transport	mol/hr	NS
BA_canal_Vmax	Maximum rate of bulk bile acid canalicular transport	mol/hr	NS (P=0.0251)
BA_uptake_Vmax	Maximum rate of bulk bile acid uptake	mol/hr	NS
CDCA_amidation_Vmax	Maximum rate of CDCA amidation	mol/hr	NS
CDCA_baso_Vmax	Maximum rate of CDCA basolateral transport	mol/hr	NS
CDCA_canal_Vmax	Maximum rate of CDCA canalicular transport	mol/hr	NS
CDCA_uptake_Vmax	Maximum rate of CDCA uptake	mol/hr	NS
CDCAamide_baso_Vmax	Maximum rate of CDCA amide conjugates basolateral transport	mol/hr	NS
CDCAamide_canal_Vmax	Maximum rate of CDCA amide conjugates canalicular transport	mol/hr	NS
CDCAamide_uptake_Vmax	Maximum rate of CDCA amide conjugates uptake	mol/hr	NS
LCA_baso_Vmax	Maximum rate of LCA basolateral transport	mol/hr	NS
LCA_canal_Vmax	Maximum rate of LCA canalicular transport	mol/hr	NS
LCA_detox_Vmax^{R}	Maximum rate of LCA hydroxylation^{R}	mol/hr	NS
LCA_synthesis_Vmax	Maximum rate of LCA synthesis from CDCA in the gut	mol/hr	NS
LCA_uptake_Vmax	Maximum rate of LCA uptake	mol/hr	NS
LCAamide_baso_Vmax	Maximum rate of LCA amide conjugates basolateral transport	mol/hr	NS
LCAamide_canal_Vmax	Maximum rate of LCA amide conjugates canalicular transport	mol/hr	NS
LCAamide_sulfation_Vmax^{H}	Maximum rate of LCA amide conjugates sulfation^{H}	mol/hr	--
LCAamide_uptake_Vmax	Maximum rate of LCA amide conjugates uptake	mol/hr	NS
LCAsulfate_baso_Vmax	Maximum rate of LCA sulfate conjugates basolateral transport	mol/hr	NS
LCAsulfate_canal_Vmax	Maximum rate of LCA sulfate conjugates canalicular transport	mol/hr	NS
LCAsulfate_uptake_Vmax	Maximum rate of LCA sulfate conjugates uptake	mol/hr	NS
canal_reg_scale	Magnitude of regulation of canalicular transporters relative to bile acid synthesis	n.d.	NS
uptake_reg_scale	Magnitude of regulation of uptake transporters relative to bile acid synthesis	n.d.	NS
	RNS/ROS toxicity submodel		
RNS_ROS_ATP_inhib_Vmax	Maximum reaction rate between reactive species and ATP production	n.d.	NS
RNS_ROS_cl_Vmax	Maximum rate for clearance of reactive	1/hr	NS

	species in the liver		
	System-specific parameters		
Body_mass	Body weight	kg	NS
ATP_decr_necrosis_Vmax	Maximum reaction rate between ATP decrement and necrosis	1/hr	NS (P = 0.0061)
HC_necr_HMGB1_release_rate[R]	Amount of HMGB1 released by necrotic cells[R]	ng/1e9 cells	NS
HGF_prod_LSEC_Vmax[H]	Maximum liver sinusoidal endothelial cell HGF production rate per liver LSEC[H]	ng/hr/1e9 cells	--
HGF_regen_Vmax[H]	Maximum rate of HGF mediated regeneration[H]	n.d.	--
GSH_pre_trans_Vmax	Maximum rate of GSH precursor transport	mol/mL/hr	NS
GSHo	GSH basal level	mol/mL	NS
CAS_apop_scale	Caspase-mediated apoptosis scaling constant	n.d.	NS
TNF_mediated_necrosis_Vmax[R]	Maximum value for allowing TNF-mediated necrosis based on ATP levels[R]	n.d.	NS

[H] human SimPops parameter only
[R] rat SimPops parameter only

Supplement Table S3. Calculated K_p and $K_{p,u}$ values. Values of K_p and $K_{p,u}$ were calculated from two different PBPK models —oral dosing and IV infusion—as liver C_{max}/plasma C_{max} and a Rodgers and Rowland estimation based on pH, pK_a, and the blood-to-plasma ratio. In the case of estimates for human K_p and $K_{p,u}$, the PBPK IV infusion and Rodgers and Rowland methods are comparable.

	PBPK oral dosing		**PBPK IV infusion**		**Rodgers and Rowland**	
	K_p	**$K_{p,u}$**	**K_p**	**$K_{p,u}$**	**K_p**	**$K_{p,u}$**
Human	15.7	1725.2747	0.082429*	9.0581*	0.09237	10.15
Rat	5.3	141.3	0.848027	22.6141	0.1125	3

*K_p and $K_{p,u}$ values used to estimate intracellular concentration for ROS and Seahorse XF96 assays, respectively, for simulating toxicity outcomes

Supplement Table S4. Mitochondrial Toxicity Parameter Translation from MITOsym to DILIsym. MITOsym was used to reproduce responses observed in HepG2 cells treated with rotenone, a known electron transport chain (ETC) inhibitor. DILIsym was used to simulate rotenone effects in humans and rats. CKA effects in HepG2 cells were then reproduced in MITOsym, and parameter values quantifying electron transport chain inhibition (ETCi) were translated from MITOsym to DILIsym using the ratio determined from the parameter values for rotenone.

	MITOsym ETCi Parameter Value (mM)	**DILIsym ETCi Parameter Value (mM)**	
	HepG2 cells	**Human**	**Rat**
Exemplar (rotenone)	2.16×10^{-5}	7.50×10^{-4}	7.50×10^{-5}
CKA	0.41	14.2	1.42